Global Combustion Mechanisms for Use in CFD Modeling under Oxy-Fuel Conditions

Jimmy Andersen, Christian Lund Rasmussen, Trine Giselsson, and Peter Glarborg*

Department of Chemical and Biochemical Engineering Technical University of Denmark, DK-2800 Kgs. Lyngby, Denmark

Received May 16, 2008. Revised Manuscript Received December 16, 2008

Two global multistep schemes, the two-step mechanism of Westbrook and Dryer (WD) and the four-step mechanism of Jones and Lindstedt (JL), have been refined for oxy-fuel conditions. Reference calculations were conducted with a detailed chemical kinetic mechanism, validated for oxy-fuel combustion conditions. In the modification approach, the initiating reactions involving hydrocarbon and oxygen were retained, while modifying the $H_2-CO-CO_2$ reactions in order to improve prediction of major species concentrations. The main attention has been to capture the trend and level of CO predicted by the detailed mechanism as well as the correct equilibrium concentration. A CFD analysis of a propane oxy-fuel flame has been performed using both the original and modified mechanisms. Compared to the original schemes, the modified WD mechanism improved the prediction of the temperature field and of CO in the post flame zone, while the modified JL mechanism provided a slightly better prediction of CO in the flame zone.

Introduction

Oxy-fuel combustion is a promising technique for separating gaseous CO_2 with the intention of storing it, for instance in geological reservoirs. The separation of CO_2 is facilitated by removing the atmospheric nitrogen from air before combustion. Recirculated combustion products are used for diluting a pure O_2 stream. Due to the higher heat capacity and radiative properties of CO_2 compared to N_2, an increased oxygen concentration is required to obtain the same thermal conditions as combustion in air. For natural gas, a mixture of 28% O_2 and 72% CO_2 will result in a temperature field similar to combustion in air.[1] Oxy-fuel combustion will eventually result in a flue gas consisting mainly of CO_2 and steam. The flue gas can then undergo a condensation process to remove the H_2O, before a part of this flue gas consisting almost entirely of CO_2 is recirculated, while the remaining part is ready for compression and storage.[2]

Computational fluid dynamics (CFD) is becoming an important industrial tool for trouble-shooting and optimization. However, CFD modeling of industrial combustion applications is a computationally demanding task. For this reason, it is often necessary to apply simplified reaction mechanisms to reduce the computing effort. Chemistry is often represented by a mixed-is-burned assumption or an assumption of chemical equilibrium. Breussin et al.[3] performed a CFD analysis of a pure natural gas/oxygen flame, and found good predictions for the fluid dynamics, temperature and main chemical species concentration fields (O_2, CO_2) using both an Eddy Dissipation/mixed-is-burned approach and an EDC/chemical equilibrium approach. The mixed-is-burned model did, however, fail in predicting CO properly. In all the flames predicted, the equilibrium model showed to be superior to the mixed-is-burned model. The temperature and species concentrations predictions were better, since the effect of molecular dissociation has been accounted for. An alternative to these approaches is to employ finite-rate chemistry, using a scheme consisting of one or several global reactions. A number of simplified methane oxidation mechanisms has been proposed in literature.[4−9] Brink et al.[10] tested this approach under perfectly stirred reactor conditions. An equilibrium approach was compared with a three-step irreversible mechanism,[10] the four-step mechanism suggested by Jones and Lindstedt[6] and a detailed mechanism suggested by Glarborg et al.[11] Their conclusions were that thermodynamic equilibrium provides a poor description under conditions with a strong coupling between turbulent mixing and chemical reactions. The global mechanisms resembled the detailed model well at fuel-lean conditions. At fuel-rich conditions, the accuracy of the three-step irreversible model was less satisfactory, whereas the four-step mechanism performed better and correctly approached the equilibrium composition at long residence times. The four-step mechanism was reported to be a good compromise between accuracy and computational effort.[10]

Examples of CFD modeling using the global mechanisms can be found in the literature.[10,12−14] Also, in industrial CFD modeling, the global mechanisms are used frequently, presum-

* To whom correspondence should be addressed. Tel: +45 4525 2840. Fax: +45 4588 2258. E-mail: pgl@kt.dtu.dk.

(1) Andersson, K.; Johnsson, F. *Fuel* **2007**, *86*, 656–688.
(2) Wall, T. F. *Proc. Combust. Inst.* **2007**, *31*, 31–47.
(3) Breussin, F.; Lallemant, N.; Weber, R. *Combust. Sci. Technol.* **2000**, *160*, 369–397.
(4) Dryer, F. L.; Glassman, I. *Proc. Combust. Inst.* **1972**, *14*, 987–1003.
(5) Westbrook, C. K.; Dryer, F. L. *Combust. Sci. Technol.* **1981**, *27*, 31–44.
(6) Jones, W. P.; Lindstedt, R. P. *Combust. Flame* **1988**, *73*, 233–249.
(7) Dupont, V.; Pourkashanian, M.; Williams, A.; J. *Inst. Energy* **1993**, *66*, 20–28.
(8) Nicol, D. G.; Malte, P. C.; Hamer, A. J.; Roby, R. J.; Steele, R. C. *J. Eng. Gas Turbines Power* **1999**, *121*, 272–280.
(9) Meredith, K. V.; Black, D. L. *44th AIAA Aerospace Sciences Meeting* **2006**, *19*, 14161–14167.
(10) Brink, A.; Kilpinen, P.; Hupa, M.; Kjaldman, L. *Combust. Sci. Technol.* **1999**, *141*, 59–81.
(11) Glarborg, P.; Alzueta, M. U.; Dam-Johansen, K.; Miller, J. A. *Combust. Flame* **1998**, *115*, 1–27.
(12) Brink, A.; Mueller, C.; Kilpinen, P.; Hupa, M. *Combust. Flame* **2000**, *123*, 275–279.

10.1021/ef8003619 CCC: $40.75
Published on Web 01/28/2009

Table 1. Westbrook and Dryer Global Multi Step Methane Combustion Mechanism with Kinetic Data (units in cm, s, cal, and mol)

mechanism	reactions	A	β	E_a	reaction orders	ref
WD1	$CH_4 + 1.5\ O_2 \rightarrow CO + 2\ H_2O$	1.59×10^{13}	0	47.8×10^3	$[CH_4]^{0.7}[O_2]^{0.8}$	4
WD2	$CO + 0.5\ O_2 \rightarrow CO_2$	3.98×10^{14}	0	40.7×10^3	$[CO][O_2]^{0.25}[H_2O]^{0.5}$	4
*WD2*r	$CO_2 \rightarrow CO + 0.5\ O_2$	5.0×10^8	0	40.7×10^3	$[CO_2]$	5

ably because the models are simple, cheap, and readily available. Furthermore, computationally simple mechanisms do provide adequate results if only the main species concentrations and the temperature picture is of interest. The simplified schemes cannot be expected, however, to work as well under oxy-fuel combustion conditions, as they do for conventional combustion. The exchange of the largely inert N_2 with a chemically reactive compound, CO_2; at least at high temperatures, has been shown to change the importance of some of the elementary reactions governing the combustion,[15] thereby requiring a modification of the global multistep reaction mechanisms to make them valid under oxy-fuel conditions.

The objective of the present work is to modify two simple multistep mechanisms, used frequently for describing conventional combustion, to handle the increased CO_2 concentration under oxy-fuel conditions. The two-step hydrocarbon oxidation mechanism by Westbrook and Dryer (WD)[5] is selected, since this scheme is directly available as default in the commercial CFD code Fluent.[16] The second scheme selected is the four-step mechanism of Jones and Lindstedt (JL).[6] The JL scheme is more complex but also has a higher accuracy and similar to the WD scheme, it is used regularly in CFD modeling of industrial applications.

The selected simplified mechanisms are compared with reference calculations, conducted with the detailed combustion mechanism proposed by Glarborg and Bentzen.[15] Their kinetic model provides good agreement with oxy-fuel combustion experiments. The work presented herein bears some resemblance to the work of Brink et al.[10] They also tested the Jones and Lindstedt four-step mechanism with reference calculations with a detailed mechanism, but only for conventional combustion conditions.

Modeling Approach. The Eddy Dissipation Concept (EDC) is a popular turbulence chemistry interaction model for CFD analysis of combustion applications. The Eddy Dissipation Concept is an extension of the Eddy Dissipation model[17] based on the work by Gran and Magnussen.[18,19] In the EDC model, chemical reactions are assumed to occur in the fine structures of the computational cells. These small scale structures can be pictured as a part of the cell, where Kolmogorov-sized eddies containing combustion species are situated so close together that mixing on the molecular level is taking place. The EDC model evaluates the volume of each cell, where mixing on a molecular scale is occurring, and treats this part of the cell as a Perfectly Stirred Reactor (PSR/CSTR). The cell volume fraction and reactor residence time is depending on turbulence parameters for the specific computational cell.[18,19]

Since the turbulence/chemistry interaction description in CFD may involve ideal reactor modeling, a comparison of the performance of different global multistep reaction mechanisms should be conducted under similar conditions. True to the concept of Gran and Magnussen,[18,19] Brink et al.[10] tested the simplified models under perfectly stirred reactor conditions. However, it is questionable whether commercial CFD codes actually employ a PSR solver for the chemistry, since the resulting algebraic equations may yield convergence problems. More likely, codes like Fluent employ a numerical solver that performs an integration in time. Consequently, in the present work, isothermal plug flow reactor (PFR) modeling, rather than PSR calculations, is used to compare the global and detailed mechanisms. Detailed model predictions have been obtained from plug flow simulations using the Senkin code from the Chemkin−II library.[20] The global multistep model PFR calculations have been performed in Matlab. Even though the Chemkin 4.0 package[21] can handle the noninteger reaction orders that are often applied in global mechanisms, the Matlab code was preferred because it facilitated comparison of several parameters for both the detailed and global models. It should be noted, however, that convergence can be problematic when using non-integer reaction coefficients and because of this, the stiff numerical solver ode15s was preferred over ordinary ODE solvers.

Detailed Chemical Kinetic Model (DCKM). In this work, the global mechanisms are compared to the detailed chemical kinetic mechanism (DCKM) presented by Glarborg and Bentzen.[15] To the authors' knowledge, this mechanism is the only one that has been validated against oxy-fuel experiments. The mechanism satisfactorily predicts CO, CO_2 and O_2 concentrations from oxidation of CH_4 by an O_2/CO_2 mixture in a flow reactor with residence times of approximately 1 s.[15]

The Westbrook and Dryer Two-Step Mechanism (WD). The WD model consists of two reactions, where the last step, oxidation of CO to CO_2, is reversible. The mechanism is listed in the form of three irreversible steps,

$$CH_4 + 1.5O_2 \rightarrow CO + 2H_2O \quad \text{(WD1)}$$

$$CO + 0.5O_2 \rightarrow CO_2 \quad \text{(WD2)}$$

$$CO_2 \rightarrow CO + 0.5O_2 \quad \text{(WD3)}$$

Table 1 displays the reaction rate data for the WD mechanism. The rate constants for (WD1) and (WD2) originate from Dryer and Glassman[4] who studied high temperature oxidation reactions of carbon monoxide and methane under fuel lean conditions ($\lambda > 2$) in a turbulent flow reactor. Later, Westbrook and Dryer[5] included the reverse reaction step for CO_2 decomposition (WD3) in order to reproduce the proper heat of reaction and pressure dependence of the $[CO]/[CO_2]$ equilibrium.

The Jones and Lindstedt Four-Step Mechanism (JL). Jones and Lindstedt[6] developed four-step global mechanisms for several hydrocarbon fuels. For methane, it involves the following steps:

$$CH_4 + 0.5O_2 \rightarrow CO + 2H_2 \quad \text{(JL1)}$$

$$CH_4 + H_2O \rightarrow CO + 3H_2 \quad \text{(JL2)}$$

$$H_2 + 0.5O_2 \rightleftarrows H_2O \quad \text{(JL3)}$$

$$CO + H_2O \rightleftarrows CO_2 + H_2 \quad \text{(JL4)}$$

The mechanism consists of two irreversible reactions, (JL1) and (JL2), describing the initial oxidation steps of a hydrocarbon. The two reversible reactions, (JL3) and (JL4), control the rate of reaction for CO and H_2. The rate coefficients for methane combustion are displayed in Table 2. Jones and Lindstedt validated the model against data for premixed methane and propane flames along with diffusion flame data for a methane-air flame. The mechanism was reported to perform well for both fuel-lean and moderately fuel-rich stoichiometries.[6] Two sets of rate parameters for reaction (JL3) were presented. Set (JL3a) was the preferred expression, but since it involved negative

Table 2. Jones Lindstedt Global Multi-Step Methane Combustion Mechanism with the Kinetic Rate Data (units in cm, s, cal, and mol)

no.	reactions	A	β	E_a	reaction orders	ref
JL1	$CH_4 + 0.5\ O_2 \rightarrow CO + 2\ H_2$	7.82×10^{13}	0	30.0×10^3	$[CH_4]^{0.5}[O_2]^{1.25}$	6
JL2	$CH_4 + H_2O \rightarrow CO + 3\ H_2$	0.30×10^{12}	0	30.0×10^3	$[CH_4][H_2O]$	6
*JL3*a	$H_2 + 0.5\ O_2 \rightleftharpoons H_2O$	4.45×10^{18}	−1	40.0×10^3	$[H_2]^{0.5}[O_2]^{2.25}[H_2O]^{-1}$	6
*JL3*b	$H_2 + 0.5\ O_2 \rightleftharpoons H_2O$	1.21×10^{18}	−1	40.0×10^3	$[H_2]^{0.25}[O_2]^{1.5}$	6
JL4	$CO + H_2O \rightleftharpoons CO_2 + H_2$	2.75×10^{12}	0	20.0×10^3	$[CO][H_2O]$	6

Table 3. Chemkin-Code for the JL Mechanism (3b H_2-O_2 Reaction) (units: cm, s, cal, mol, and K)

ELEMENTS C O H N END				
SPECIES CH4 O2 H2O N2 CO CO2 H2 END				
REACTIONS				
CH4 + 0.5 O2 = > CO+ 2H2	7.82×10^{13}	0	30.0×10^3	!Jones Lindstedt 88
FORD /CH4 0.5/				
FORD /O2 1.25/				
CH4 + H2O = > CO + 3H2	0.30×10^{12}	0	30.0×10^3	!Jones Lindstedt 88
H2 + 0.5 O2 = > H2O	1.209×10^{18}	−1	40.0×10^3	!Jones Lindstedt 88
FORD /H2 0.25/				
FORD /O2 1.5/				
H2O + 0 O2 +0 H2 = > H2 + 0.5 O2	7.06×10^{17}	−0.877	97.9×10^3	!Calculated
FORD /H2 −0.75/				
FORD /O2 1/				
FORD /H2O 1/				
CO + H2O = CO2+H2	0.275×10^{13}	0	20.0×10^3	!Jones Lindstedt 88
END				

reaction orders that might cause numerical problems, the set for (JL3b) was proposed as an alternative.[6]

If (JL3) had been an elementary reaction, the reverse rate constant could be determined from expression 1,

$$\frac{\dot{R}_{JL3,f}}{\dot{R}_{JL3,r}} = K_{JL3} = \frac{k_{JL3,f}[H_2][O_2]^{0.5}}{k_{JL3,r}[H_2O]} \quad (1)$$

Here, K_{JL3} is the equilibrium constant, k_{JL3} is the rate constant, and the f and r subscribts refer to the forward and reverse reactions, respectively. However, (JL3) is a global reaction and the forward reaction orders do not follow the stoichiometry. For this reason, the reverse reaction order for reaction (JL3a) or (JL3b) cannot be derived according to eq 1. In order for an equilibrium approach to be maintained for a global reaction, the expression 1 must still hold at equilibrium, here exemplified with reaction (JL3b):

$$\frac{\dot{R}_{JL3,f}}{\dot{R}_{JL3,r}} = \frac{\dot{R}^*_{JL3b,f}}{\dot{R}^*_{JL3b,r}} = \frac{k_{JL3,f}[H_2][O_2]^{0.5}}{k_{JL3,r}[H_2O]} = \frac{k^*_{JL3b,f}[H_2]^{0.25}[O_2]^{1.5}}{k^*_{JL3b,r}[H_2O]} \quad (2)$$

The superscript * refers to the global rate expressions. Since the forward rate constant for the global and the stoichiometric expression, respectively, must be identical ($k_{JL3,f} = k^*_{JL3b,f}$), the concentration dependence of the reverse reactions can be found as follows:

$$k^*_{JL3b,r} = k_{JL3,r}[H_2]^{-0.75}[O_2] \Rightarrow \dot{R}^*_{JL3b,r} = k_{JL3,r}[H_2]^{-0.75}[O_2][H_2O] \quad (3)$$

In the present work, the derivation of the backward rates is done by evaluating the forward rates divided by the equilibrium constant at a series of temperatures (from 500 to 2500 K with 100 K increments) and then fitting an Arrhenius expression to the results, to obtain an individual expression for the reverse reaction. For reaction (JL3a) we obtain the expression,

$$k^*_{JL3a,r}(T) = 2.6 \times 10^{18} \cdot T^{-0.877} \cdot \exp\left(-\frac{49260}{T}\right) \quad (4)$$

and for reaction (JL3b),

$$k^*_{JL3b,r}(T) = 7.1 \times 10^{17} \cdot T^{-0.877} \cdot \exp\left(-\frac{49260}{T}\right) \quad (5)$$

These expressions make it possible to implement the forward and reverse reactions as irreversible steps, facilitating the use in commercial CFD software such as Fluent.[16]

In the following, only reaction 3b of the JL mechanism is used. Attempts to use 3a resulted in problems with convergence which may limit its use in CFD. Another concern related to 3a is that the reverse rate for (JL3a) is independent of the H_2O concentration. This makes sense when the purpose of the reaction is to dampen the forward reaction, but under conditions with large H_2O concentrations or even H_2O in the oxidizer stream a zero reaction order may be inappropriate.

A way to implement the JL mechanism in Fluent[16] is to import it as a Chemkin input file. In the newer versions of Chemkin, the FORD keyword is used to overwrite the forward reaction order, allowing global expressions to be implemented. Table 3 shows an example of a Chemkin input file, with reaction (3b) implemented. Note that in the reverse H_2-O_2 reaction, H_2 and O_2 have been added as reactants with 0 as stoichiometry coefficients. This is required to allow the program to overwrite the forward reaction orders.

Results and Discussion

In this work, we evaluate the performance of the WD and JL schemes under conditions of conventional combustion and oxy-fuel combustion, respectively, assuming plug-flow. Then the two schemes are revised for use under oxy-fuel conditions and tested again against reference calculations with the detailed mechanism. Finally, the original and modified schemes are implemented and compared for CFD calculations of a turbulent diffusion propane/O_2/CO_2 flame under conditions similar to those reported recently by Andersson and Johnsson.[1]

Performance of the WD and JL Mechanisms. Both the JL and the WD global mechanisms have been used extensively in CFD models for conventional combustion in air. Before we investigate how the schemes function under oxy-fuel conditions, we test them under normal combustion conditions by comparing with reference calculations with the detailed reaction mechanism. Since the mechanisms were optimized for fuel-lean conditions, we evaluate them at conditions with excess air.

Figure 1 compares CO, O_2 and CO_2 concentrations in an isothermal plug flow reactor at 1600 K and an excess air ratio

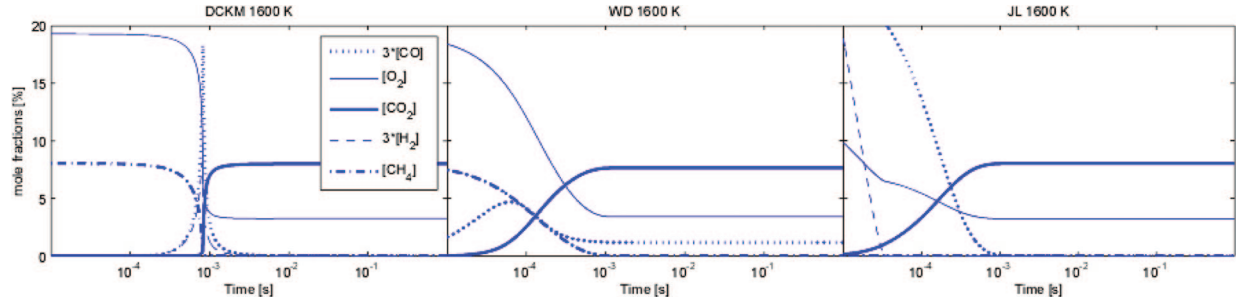

Figure 1. Major species concentrations in plug flow calculations. Comparison between the DCKM, the WD and the JL mechanisms at $\lambda = 1.2$ and 1600 K under "air" firing conditions (21% O_2 and 79% N_2).

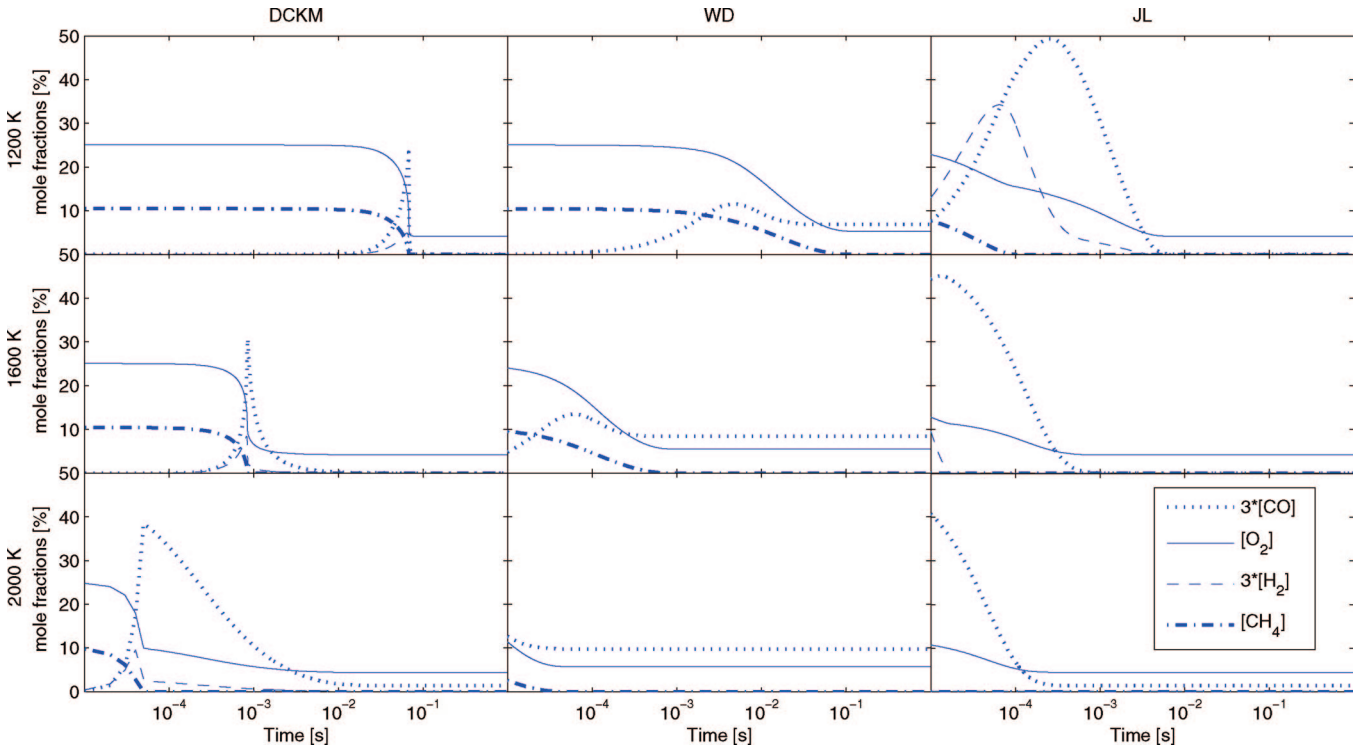

Figure 2. Major species concentrations in plug flow calculations. Comparison between the DCKM, the WD, and the JL mechanisms at $\lambda = 1.2$ and 1200 K (top), 1600 K (middle), and 2000 K (bottom) under "oxy"-firing conditions (28% O_2 and 72% CO_2).

of $\lambda = 1.2$. These results, along with other simulations, show that both the WD and JL mechanisms adequately predict O_2 and CO_2 levels at fuel lean conditions. Thereby, they would also yield a satisfactory prediction of the heat release for nonisothermal conditions at these stoichiometries. Only the JL mechanism predicts CO correctly at longer times under fuel lean conditions. The WD mechanism tends to overpredict the CO exit concentration and may not be sufficiently accurate for CO emission modeling.

As expected, the results show differences in the predicted ignition time between the three models. Only the detailed model can describe the slow build-up of the radical pool that eventually lead to ignition in a plug-flow calculation. The global schemes cannot account for an ignition delay. The WD mechanism was developed to describe the postignition fuel-consumption rate in PFR experiments, whereas the JL mechanism was optimized for flame conditions, where a radical pool is available through diffusional processes. It is difficult to assess how inaccuracies in the description of ignition affect a CFD calculation. In the EDC approach, PSR/PFR reactor residence times may be in the range of 10^{-4} to 10^{-3} s, i.e., time scales where there are considerable differences between modeling predictions. However, all three models predict the time scale for complete conversion of CH_4 to CO_2 to be of the order of 10^{-3} s, which is satisfactory.

The performances of the WD and JL mechanisms under fuel-lean oxy-firing conditions are displayed in Figures 2 and 3. At low temperatures (<1300 K) consumption of CO_2 is practically negligible,[15] and CO_2 is expected to have little chemical effect under these conditions. At higher temperatures, such as in the figures, atomic hydrogen may start to convert CO_2 to CO, resulting in a change in both the CO/CO_2 ratio and the composition of the O/H radical pool compared to conventional combustion. In general, the level of agreement between the global mechanisms and the reference calculations is similar to that observed under conventional combustion conditions. As expected, the WD mechanism cannot predict the CO exit concentration accurately; differences are seen at all temperatures. With the exception of the ignition timing, predictions of the JL mechanism generally compare well with those of the detailed mechanism. The ability of the JL scheme to compensate for the water−gas shift reaction (JL4) allows it to capture most changes caused by the elevated CO_2 concentration. Consequently, it predicts correct levels for all major species at longer reaction times, even under fuel-rich conditions. However, the CO peak levels are overpredicted in most cases.

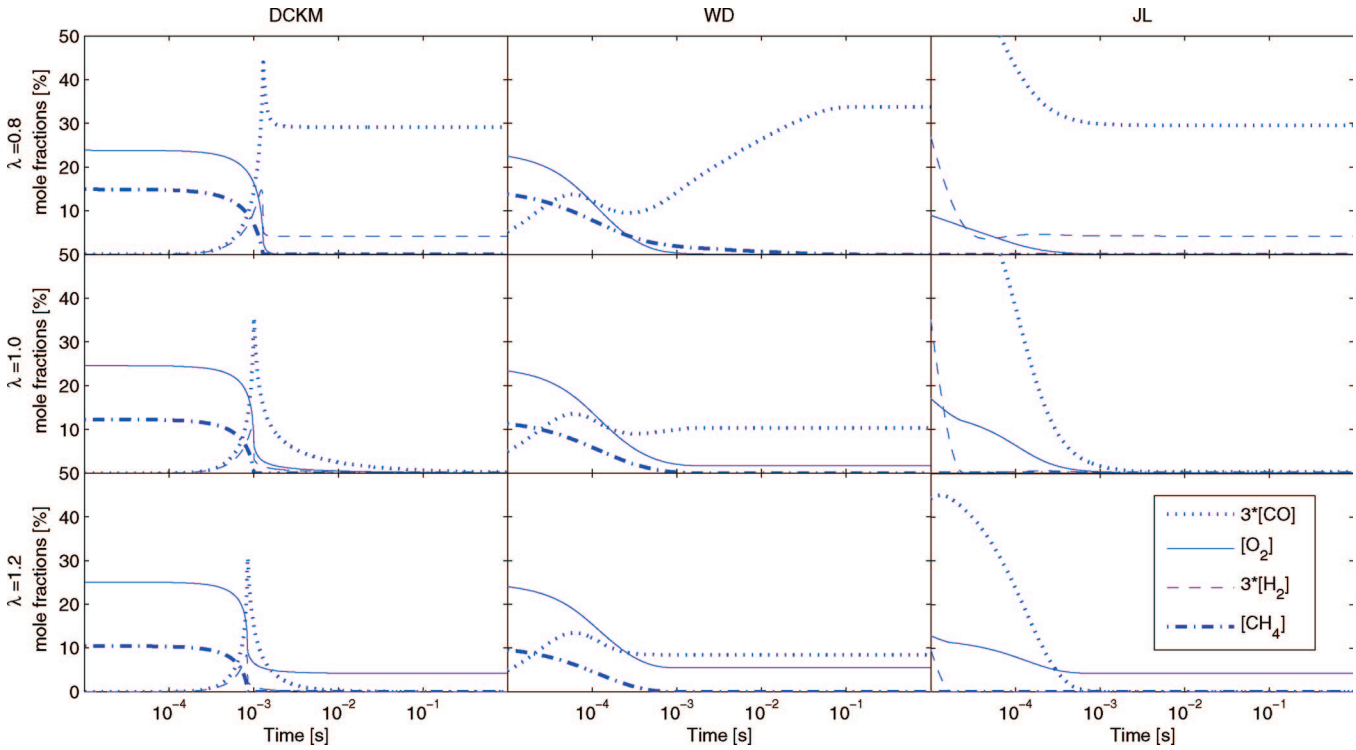

Figure 3. Major species concentrations in plug flow calculations. Comparison between the DCKM, the WD and the JL mechanisms at 1600 K and $\lambda = 0.8$ (top), $\lambda = 1.0$ (middle), and $\lambda = 1.2$ (bottom) under "oxy"-firing conditions (28% O_2 and 72% CO_2).

Table 4. Modified Multi Step Methane Combustion Mechanisms with Kinetic Rate Data - units in cm, s, cal, mol

reaction number	reactions	A	β	E_a	reaction orders
WD1	$CH_4 + 1.5\ O_2 \rightarrow CO + 2\ H_2O$	1.59×10^{13}	0	47.8×10^3	$[CH_4]^{0.7}[O_2]^{0.8}$
WD2(modified)	$CO + 0.5\ O_2 \rightarrow CO_2$	3.98×10^8	0	10.0×10^3	$[CO][O_2]^{0.25}[H_2O]^{0.5}$
WD3(modified)	$CO_2 \rightarrow CO + 0.5\ O_2$	6.16×10^{13}	−0.97	78.4×10^3	$[CO_2][H_2O]^{0.5}[O_2]^{-0.25}$
JL1	$CH_4 + 0.5\ O_2 \rightarrow CO + 2\ H_2$	7.82×10^{13}	0	30.0×10^3	$[CH_4]^{0.5}[O_2]^{1.25}$
JL2	$CH_4 + H_2O \rightarrow CO + 3\ H_2$	3.00×10^{11}	0	30.0×10^3	$[CH_4][H_2O]$
JL3(modified)	$H_2 + 0.5\ O_2 \rightarrow H_2O$	5.0×10^{20}	−1	30.0×10^3	$[H_2]^{0.25}[O_2]^{1.5}$
JL3 reverse	$H_2O \rightarrow H_2 + 0.5\ O_2$	2.93×10^{20}	−0.877	97.9×10^3	$[H_2]^{-0.75}[O_2][H_2O]$
JL4	$CO + H_2O \rightleftarrows CO_2 + H_2$	2.75×10^{12}	0	20.0×10^3	$[CO][H_2O]$

Refined Schemes for Oxy-Fuel Combustion. It is apparent that the WD mechanism needs improvement to become applicable for oxy-fuel conditions due to the poor CO prediction. The JL mechanism works satisfactorily under oxy-fuel conditions, even though the prediction of the peak CO levels could be improved. In the present work, both global models are modified to improve the prediction of the steady state concentrations and the CO trends compared to the reference calculations.

The global mechanisms, refined for oxy-fuel conditions, are summarized in Table 4. The following criteria were employed in the modification procedure:

• In time, the concentrations should approach correctly the chemical equilibrium values.

• The peak CO concentrations should approximate the values predicted by the detailed model.

The modification window involved temperatures of 1200−2000 K and stoichiometries in the range $0.8 < \lambda < 1.5$.

In the WD scheme, the major issue was the rate coefficients for reaction (WD3), which did not secure an approach to equilibrium values for CO and CO_2. These were consequently modified by applying the global mechanism equilibrium approach for the CO−CO_2 reaction, following the procedure discussed above (see eqs 2−5). This change caused the WD scheme to predict the approach to equilibrium correctly, but resulted in an underprediction of CO at higher temperatures. To improve the CO prediction, it was necessary also to modify (WD2). Consequently, both the A-factor and the activation energy for (WD2) was lowered to match better the detailed model predictions.

When comparing the CO levels predicted by the JL mechanism with the detailed mechanism, it was observed that besides the difference in ignition timing, the peak CO levels deviated, most pronounced under oxy-fuel conditions (Figures 2 and 3). The predicted CO oxidation rate in the JL scheme is governed by the reaction with water vapor (JL4). Examination of the mechanism showed that it was the availability of H_2O (formed in reaction JL3), as well as the rate constant for (JL4), that limited the CO oxidation rate. Attempts to modify the JL4 rate constant proved unsuccesful; a decrease in k_{JL4} resulted in undesired changes at some conditions (prolonged burnout period), whereas an increase had little effect, since the formation

(13) Mueller, C.; Brink, A.; Kilpinen, P.; Hupa, M.; Kremer, H. *Clean Air* **2002**, *3*, 145–163.
(14) Saario, A.; Oksanen, A. *Energy Fuels* **2008**, *22*, 297–305.
(15) Glarborg, P.; Bentzen, L. L. B. *Energy Fuels* **2007**, *22*, 291–296.
(16) Fluent 6.2 users guide, Fluent Inc., Centerra Resource Park, 10 Cavendish Court, Lebanon, NH 03766, 2005.
(17) Magnussen, B. F.; Hjertager, B. H. *Proc. Combust. Inst.* **1971**, *13*, 649–657.
(18) Gran, I.; Magnussen, B. F. *Combust. Sci. Technol.* **1996**, *119*, 171–190.
(19) Gran, I.; Magnussen, B. F. *Combust. Sci. Technol.* **1996**, *119*, 191–217.
(20) Lutz, A. E.; Kee, R. J.; Miller, J. A.;*Senkin: A Fortran Program for Predicting Homogeneous Gas Phase Chemical Kinetics With Sensitivity Analysis*, Report No. SAND87−8248 Laboratories, 1990.

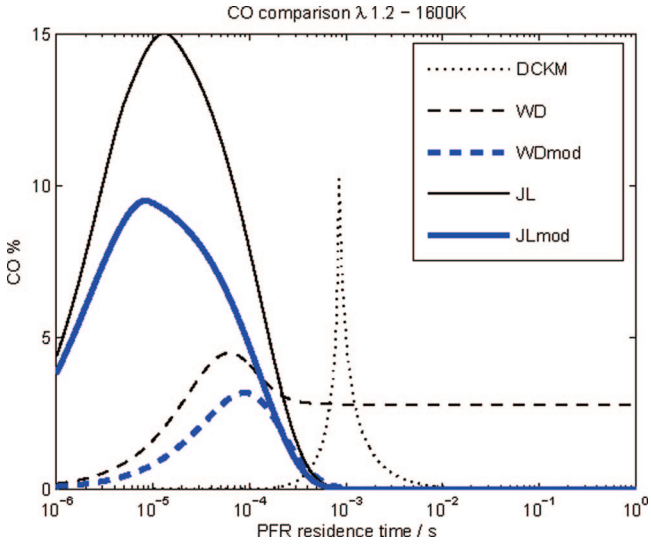

Figure 4. CO concentrations in plug flow calculations. Comparison between the DCKM, WD, JL, and modified mechanisms at 1600 K and $\lambda = 1.2$ under "oxy"-firing conditions (28% O_2 and 72% CO_2).

of H_2O (through JL3) became rate limiting. Consequently, predictions with the JL scheme were improved by modifying the rate coefficients for JL3, increasing the pre-exponential factor and decreasing the activation energy.

The parameters for the fuel-specific reactions were not part of the modification procedure; the kinetic data for the initiating reactions, i.e., (JL1), (JL2) and (WD1), were all retained. This is consistent with the flow reactor results of Glarborg and Bentzen[15] that indicate that the temperature for the initiation of reaction are very similar for reactive flows with and without CO_2. This implies that the main chemical difference between combustion in O_2/N_2 and O_2/CO_2 relates to the CO/H_2 reaction subset. Since the fuel-specific steps have been retained, the proposed schemes can easily be modified to describe higher hydrocarbons by adopting the appropriate rate data from the original mechanisms.[4,6] However, the inability of the global schemes to predict ignition timing has not been addressed.

PFR Tests of the Refined Schemes. The impact of the modifications on the CO prediction is illustrated in Figure 4 for lean conditions and 1600 K. The modification of the WD mechanism results in an improved prediction of the exit CO concentration, while the peak value is slightly lowered. The modified JL mechanism predicts a reduced peak CO level, due to the increased value of k_{JL3}. The major species concentrations predicted by the modified mechanisms are displayed in Figures 5 and 6. The results confirm that the modified schemes constitute an improvement over the WD and JL mechanisms for oxy-fuel conditions. Compared to the original schemes, the prediction in particular of the CO concentration has been improved. The improvement is most pronounced for the WD mechanism, which now predicts both the trend in CO and the approach to equilibrium concentrations reasonably well. For the modified JL mechanism, the predictions of the CO trend and the peak CO levels have been improved. Under fuel-rich conditions, both modified mechanisms approach steady-state concentrations reasonably well, as shown in Figure 6. This indicates that the schemes may be applied also for modeling staged or slightly understoichiometric combustion applications.

Figure 7 shows the performance of the modified global mechanisms when simulating a recirculated flue gas containing H_2O as well as CO_2; an option considered for oxy-fuel-fired power plants. Calculations were conducted for an oxidizer stream consisting of 28% O_2, 40% CO_2 and 32% H_2O instead of the 28% O_2 and 72% CO_2. The results confirm that the modified schemes predict the major species concentrations fairly well also under these conditions.

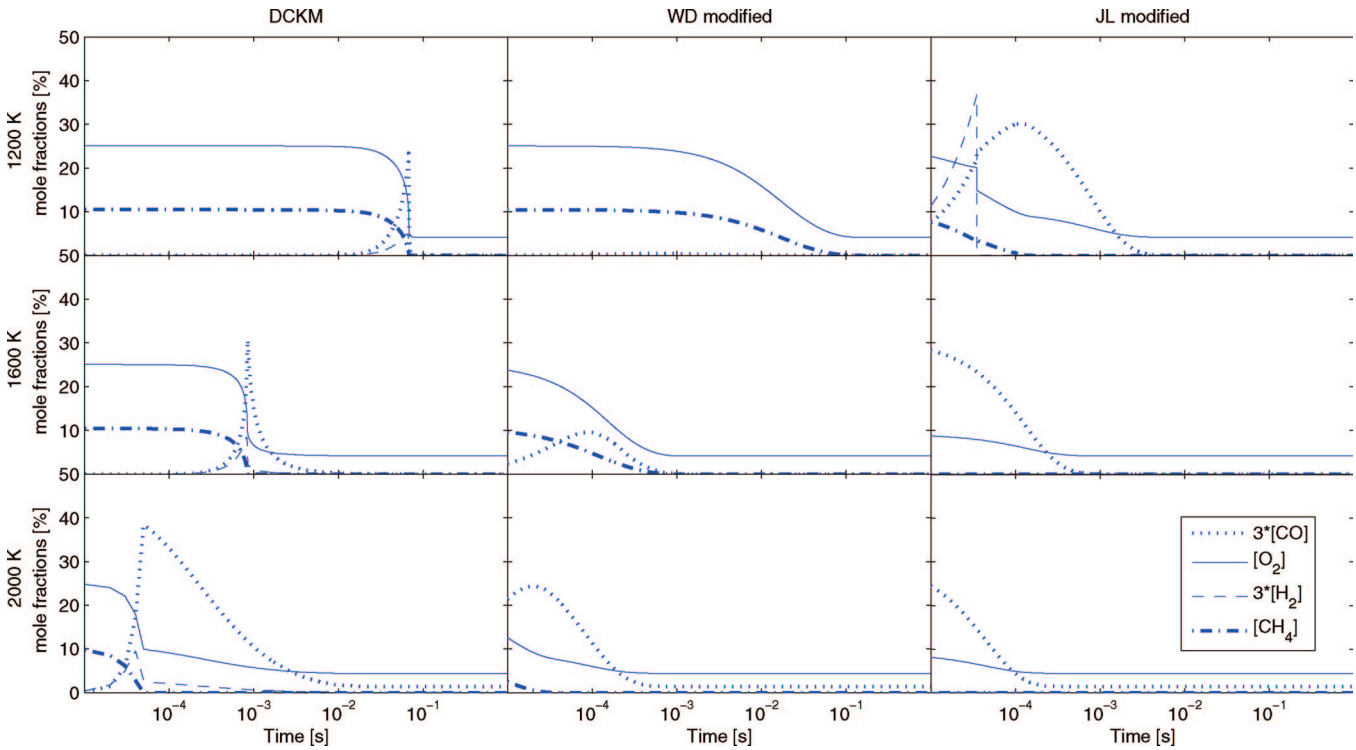

Figure 5. Major species concentrations in plug flow calculations. Comparison between the DCKM, the modified WD and the modified JL mechanisms at $\lambda = 1.2$ and 1200 K (top), 1600 K (middle), and 2000 K (bottom) under "oxy"-firing conditions (28% O_2 and 72% CO_2).

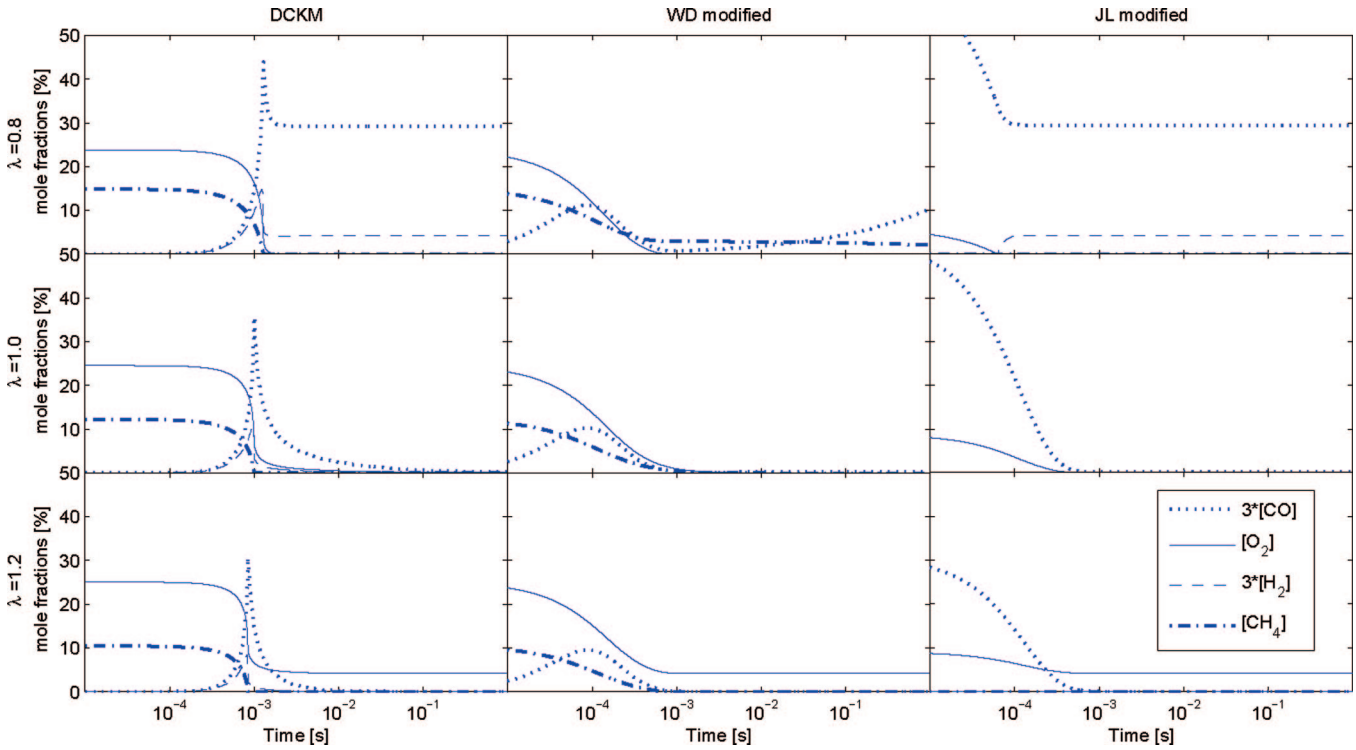

Figure 6. Major species concentrations in plug flow calculations. Comparison between the DCKM, the modified WD and the modified JL mechanisms at 1600 K and $\lambda = 0.8$ (top), $\lambda = 1.0$ (middle), and $\lambda = 1.2$ (bottom) under "oxy"-firing conditions (28% O_2 and 72% CO_2).

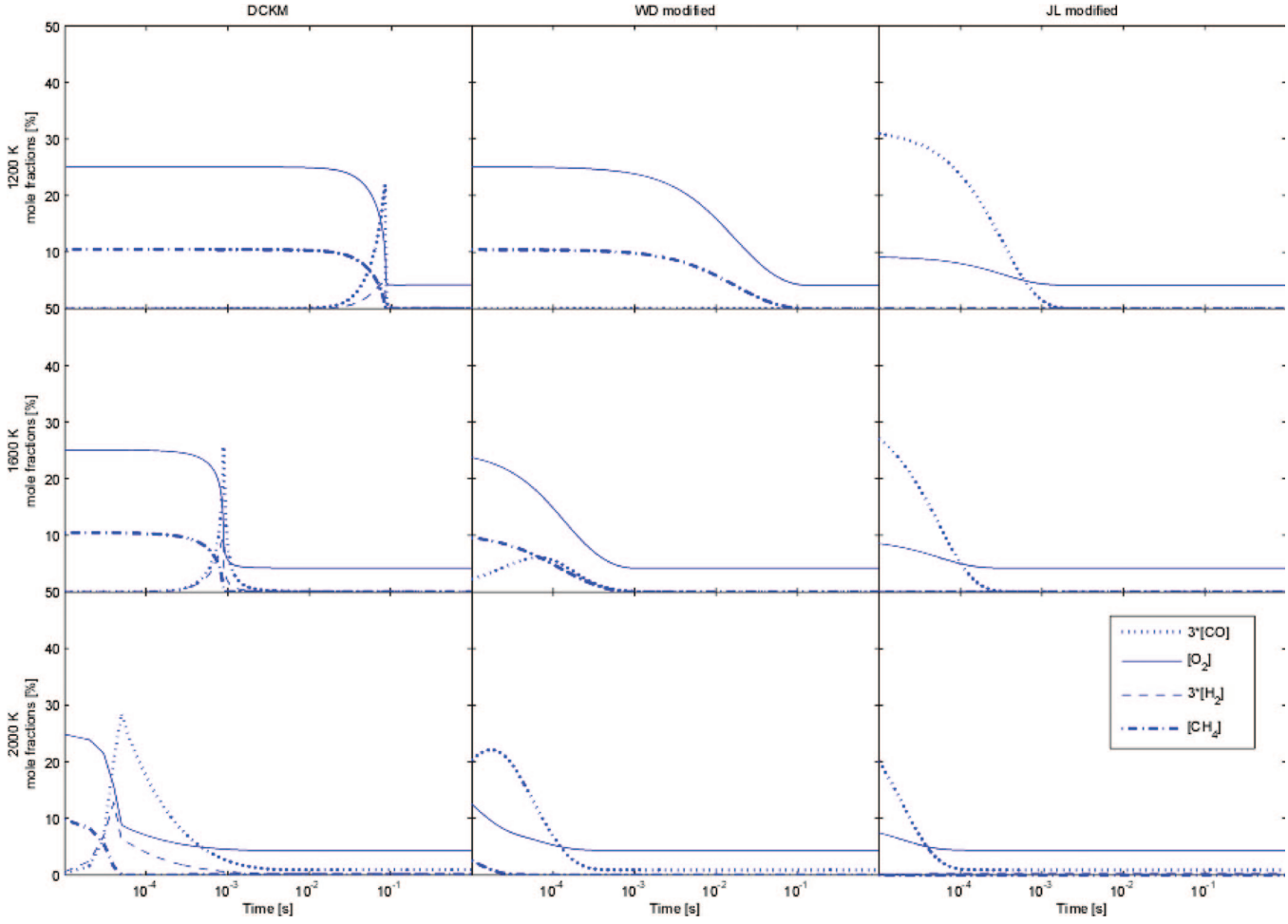

Figure 7. Major species concentrations in plug flow calculations at 1600 K. Comparison between the modified WD, JL, and detailed mechanisms under "oxy"-firing conditions with an oxidizer stream of 28% O_2, 40% CO_2 and 32% H_2O.

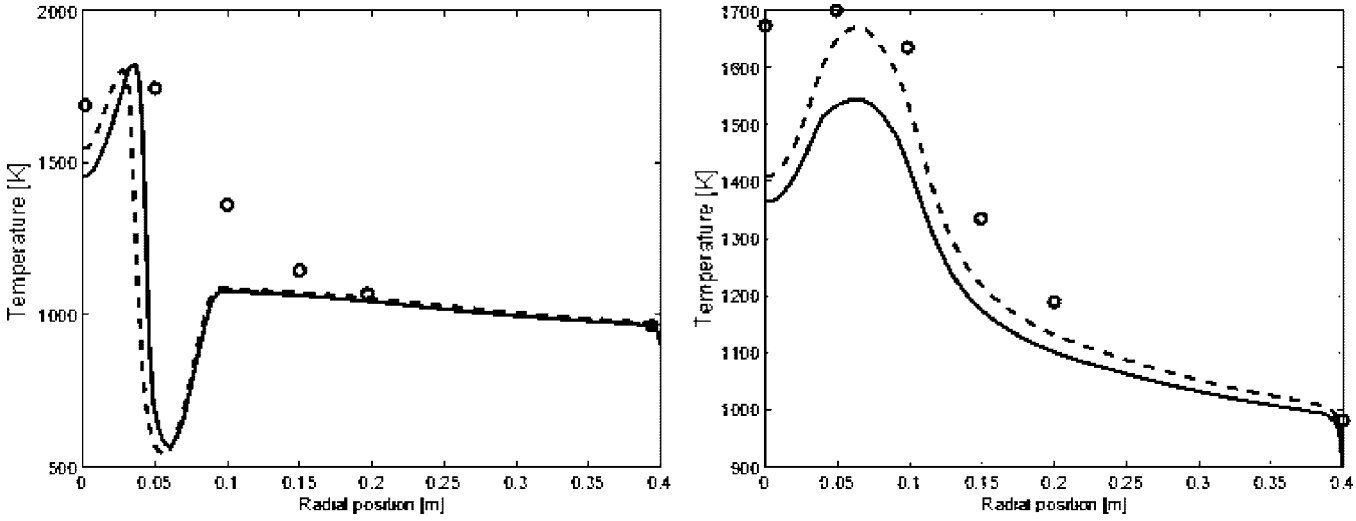

Figure 8. Temperature [K] Left: at 21.5 cm downstream of the burner. Right: at 38.4 cm downstream of the burner. Dots: Experimental data from Andersson and Johnsson.[1] Dashed line: Modified WD mechanism. Solid line: Original WD mechanism.

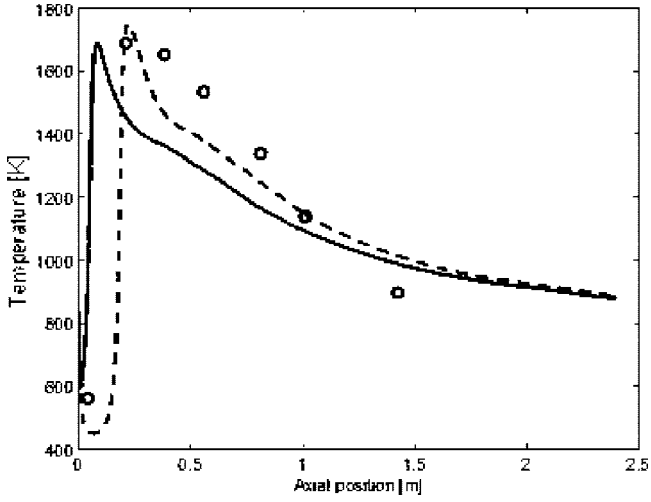

Figure 9. Temperature [K] Axial temperature at the centerline of the setup. Dots: Experimental data from Andersson and Johnsson.[1] Dashed line: Modified WD mechanism. Solid line: Original WD mechanism.

Table 5. Submodels and settings for the CFD analysis

grid	turbulence	radiation	chemistry interaction	mechanisms
2D 30.000 cells	realizable $k-\varepsilon$	P1	Eddy Dissipation concept	modified (Table *3*) original JL and WD (Tables *1*,*2*)

The turbulent mixing time scales applied in the individual CFD cells are of the order of 0.1−100 ms.[22] As expected, the modified mechanisms do not match the detailed mechanism on the smaller timescales. This implies that the global schemes have a limited accuracy in describing changes occurring on a small time scale or on an individual cell basis in a CFD computation. However, in terms of larger time scales or larger cell areas, the global mechanisms are capable of predicting satisfactorily the heat release and major species concentrations, provided the turbulence modeling provides accurate turbulence level predictions as input for the EDC turbulence chemistry interaction model.

CFD Modeling with the Refined Schemes. Recently, Andersson and Johnsson[1] reported measurements in a turbulent diffusion flame operated under oxy-fuel conditions. The experimental setup consisted of a 100 kW down-fired refractory lined furnace, with a swirl burner configuration. The fuel used was propane and the oxy-fuel experiments (27% oxygen in CO_2) were compared with data obtained in air. As part of the evaluation of the global schemes, we have conducted a CFD analysis the oxy-fuel flame. The geometry of the setup was simplified to a 2D case, even though the setup was not entirely axi-symmetric, due to four cooling tubes near the furnace walls. The heat loss to the cooling tubes was accounted for by applying a piecewise constant wall temperature to obtain gas temperatures near the walls in agreement with measurements. The grid was constructed with ∼30.000 cells. A grid-independency check indicated that this grid size was sufficient.

The commercial CFD code Fluent was used for the calculation. The realizable $k-\varepsilon$ turbulence model was adopted along with the P1 radiation model. Second-order upwind discretization was used for all transported scalars. The CFD settings are summarized in Table 5. Both the Eddy Dissipation Model (EDM) and the Eddy Dissipation Concept (EDC) were applied in the modeling of the oxy-fuel flame. We recommend to use the EDC turbulence chemistry interaction model, when modeling oxy-fuel flames. The traditional "mixed-is-burned" approach offered by the EDM is not likely to be applicable in reaction systems where reverse reactions play an important role, as is the case under oxy-fuel conditions due to CO_2 decomposition at high temperatures. Limitations of the EDM model are discussed in more detail by Brink et al.[12]

The CFD results presented here were all performed using the EDC turbulence-chemistry interaction model, applying both the original WD and JL mechanisms and the modified versions suggested in Table 4. Since the fuel used in the experiments is propane, rate data and stoichiometric relationships for the initiating reactions (JL1, JL2, and WD1, see Table 4) were modified according to the original references.[4,6] These reactions are identical in the original and modified versions.

(21) Kee, R. J.; Rupley, F. M.; Miller, J. A.; Coltrin, M. E.; Grcar, J. F.; Meeks, E.; Moffat, H. K.; Lutz, A. E.; Dixon-Lewis, G.; Smooke, M. D.; Warnatz, J.; Evans, G. H.; Larson, R. S.; Mitchell, R. E.; Petzold, L. R.; Reynolds, W. C.; Caracotsios, M.; Stewart, W. E.; Glarborg, P.; Wang, C.; Adigun, O.; Houf, W. G.; Chou, C. P.; Miller, S. F.; Ho, P.; Young, D. J.; CHEMKIN Release 4.0, Reaction Design, Inc., San Diego, CA (2004).

(22) Kjaldman, L.; Brink, A.; Hupa, M. *Combust. Sci. Technol.* **2000**, *154*, 207–227.

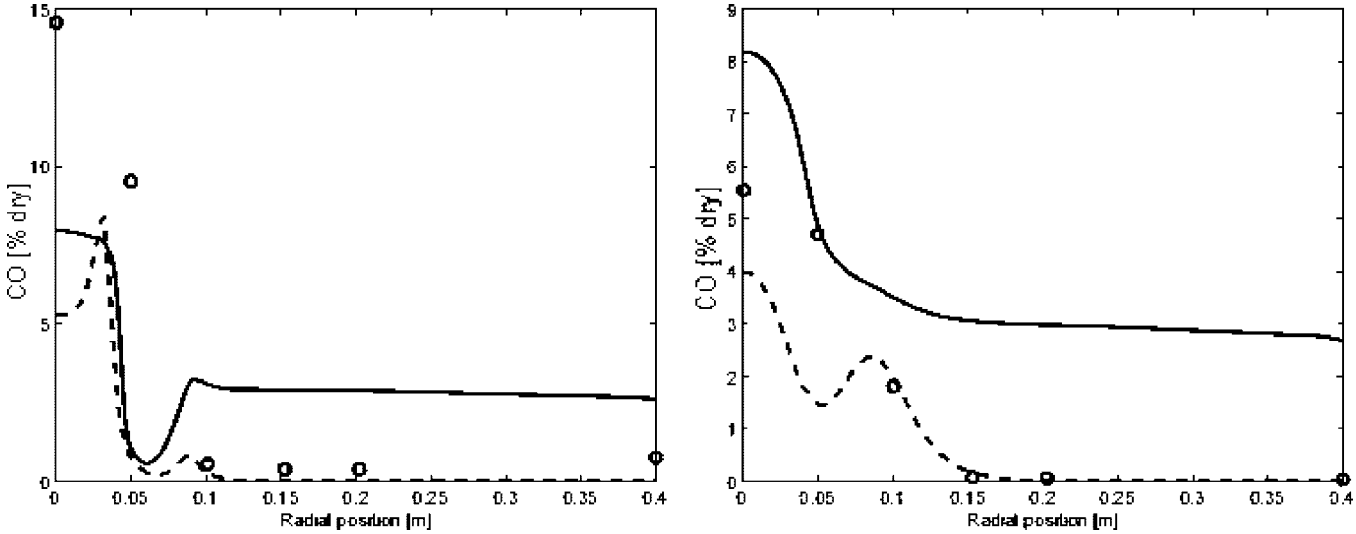

Figure 10. Radial CO concentration (%dry) Left: at 21.5 cm downstream of the burner. Right: at 38.4 cm downstream of the burner. Dots: Experimental data from Andersson and Johnsson.[1] Dashed line: Modified WD mechanism. Solid line: Original WD mechanism.

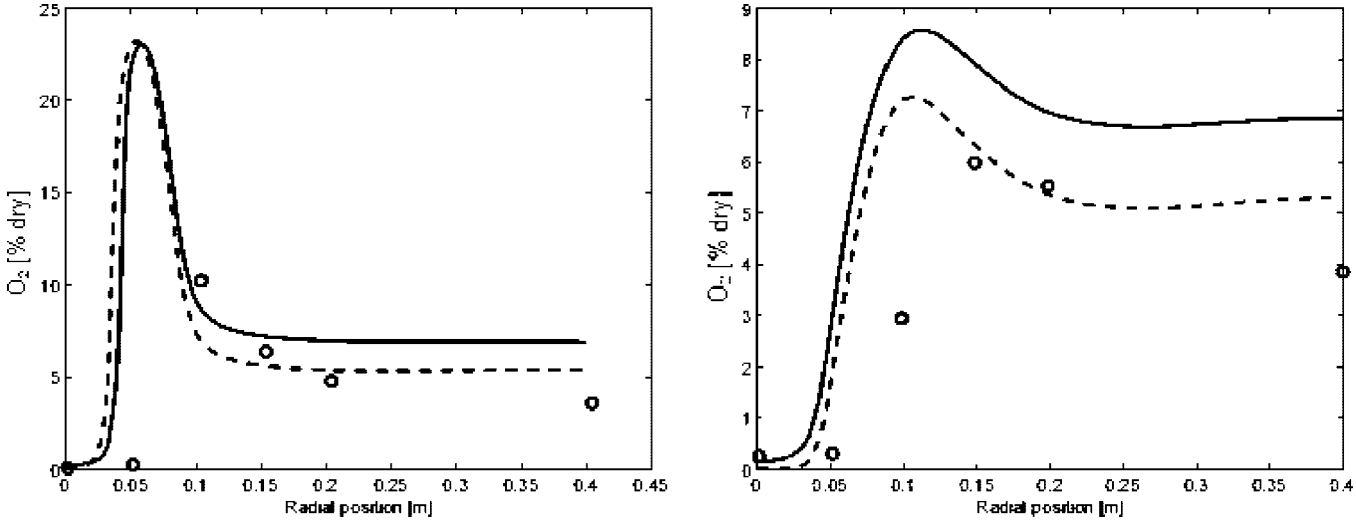

Figure 11. Radial O_2 concentration (%dry) Left: at 21.5 cm downstream of the burner. Right: at 38.4 cm downstream of the burner. Dots: Experimental data from Andersson and Johnsson.[1] Dashed line: Modified WD mechanism. Solid line: Original WD mechanism.

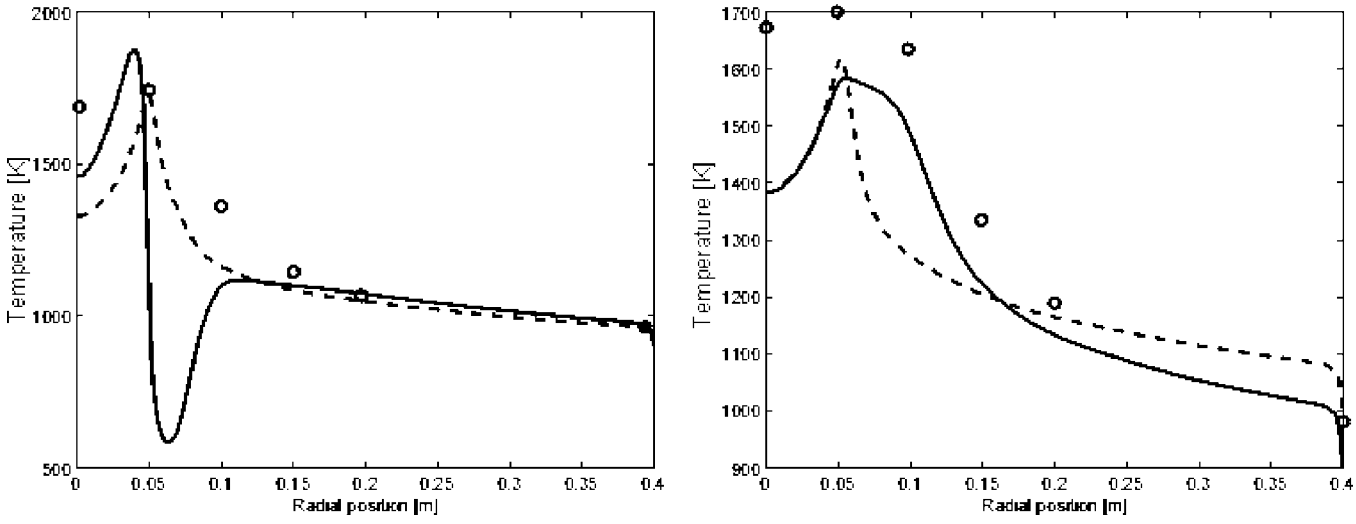

Figure 12. Temperature [K] Left: at 21.5 cm downstream of the burner. Right: at 38.4 cm downstream of the burner. Dots: Experimental data from Andersson and Johnsson.[1] Dashed line: Modified JL mechanism. Solid line: Original JL mechanism.

A satisfactory agreement between major species concentrations predicted by the CFD model and experimental results was achieved for the air case. Here, only results from the oxy-fuel case is presented. It should be noted that deviations

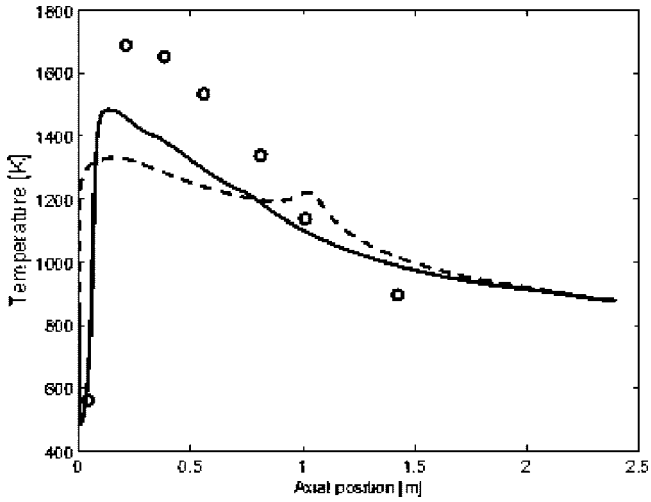

Figure 13. Temperature [K] Axial temperature at the centerline of the setup. Dots: Experimental data from Andersson and Johnsson.[1] Dashed line: Modified JL mechanism. Solid line: Original JL mechanism.

between the CFD predictions and the experimental results can only partly be attributed to an insufficient combustion mechanism. A satisfactory prediction of turbulence and flow field is essential; unfortunately, no data for velocity and velocity fluctuations are available from the oxy-fuel experiments. Radiative properties are also affected when changing from air to oxy-fuel combustion, and it is likely that differences in the temperature profiles are due to insufficient radiative modeling along with the simplifications in geometry (neglection of the cooling tubes). Furthermore, soot formation, which is important for the flame radiation, was not accounted for in the modeling.

Figures 8 and 9 show comparison between experimental results[1] and modeling predictions with the WD schemes for the radial and centerline temperature profiles, respectively, while Figures 10 and 11 show results for radial CO and O_2 concentrations. The CO and O_2 concentrations are shown for two measurement planes, 21.5 and 38.4 cm downstream of the burner. Solid lines denote calculations with the original WD scheme, while dashed lines donte predictions with the modified WD scheme. In general, the modified WD mechanism provides an improved prediction of both the temperature and the postflame conditions and emissions, compared to the original scheme. The modified mechanism predicts well the CO levels in the region outside the flame zone (Figure 10). The improvement can be attributed to the new equilib-

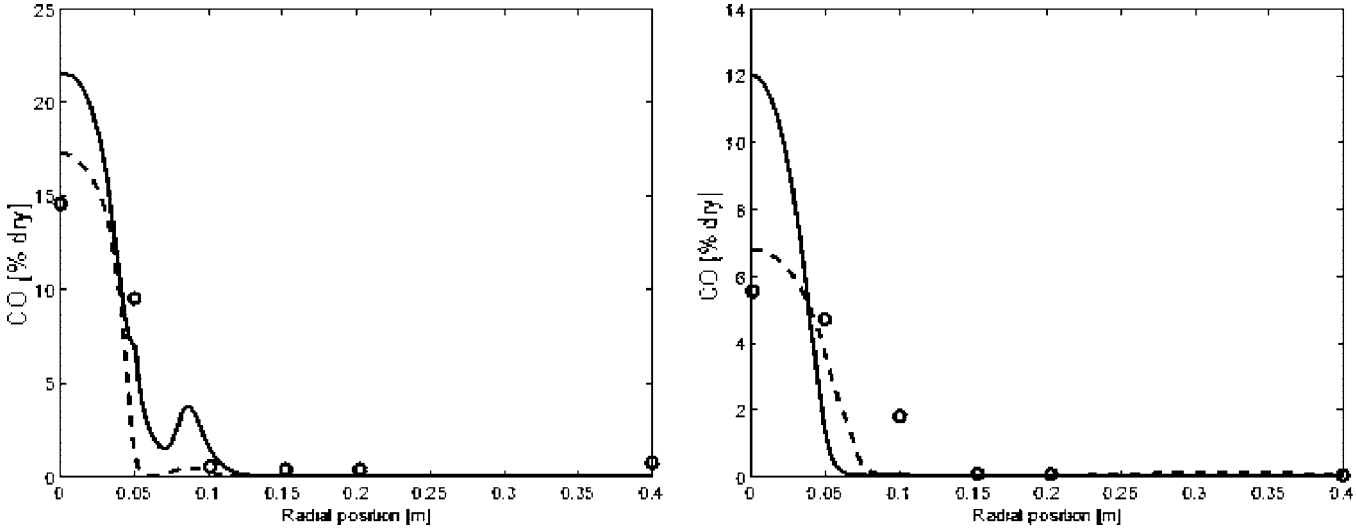

Figure 14. Radial CO concentration (%dry) Left: at 21.5 cm downstream of the burner. Right: at 38.4 cm downstream of the burner. Dots: Experimental data from Andersson and Johnsson.[1] Dashed line: Modified JL mechanism. Solid line: Original JL mechanism.

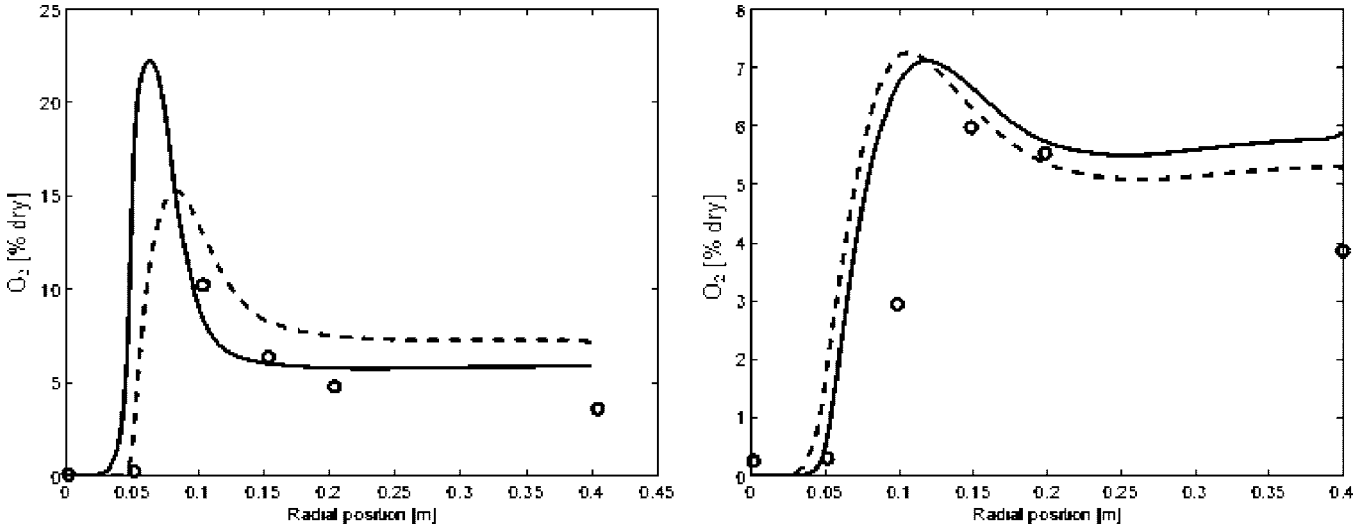

Figure 15. Radial O_2 concentration (%dry) Left: at 21.5 cm downstream of the burner. Right: at 38.4 cm downstream of the burner. Dots: Experimental data from Andersson and Johnsson.[1] Dashed line: Modified JL mechanism. Solid line: Original JL mechanism.

rium fit for the WD3 reaction. The modified model also predicts a different CO level in the flame zone, but due to the limited experimental data points for CO in this region, both sets of predictions are considered to be within experimental uncertainty. The differences in the predicted CO levels do, however, emphasize the importance of the chemical mechanism in the CFD computation. In the very fuel-rich parts of the flame, the CO levels are underpredicted in this CFD analysis. This indicates that it may be necessary to apply a more complex model than the WD scheme for reliable modeling of fuel-rich regions of a combustion system.

Comparisons for temperature profiles (Figures 12 and 13) and CO/O_2 concentrations prediction (Figures 14 and 15) have also been conducted for the JL schemes. Figures 14 and 15 compare CO and O_2 concentrations from the original JL mechanism and the modified mechanism with the experimental measurements at two measurement planes 21.5 and 38.4 cm downstream of the burner. From Figure 14, it can be seen that the modified JL mechanism predicts a lower CO concentration in the center of the furnace inside the flame, improving the agreement with experiment. The prediction of a lower CO level by the modified scheme is consistent with the PFR calculations discussed above. The modifications in the JL mechanism also induce changes in the temperature predictions (Figures 12 and 13) and the O_2 prediction (Figure 15), but whether these changes constitute improvements over the original mechanism cannot be concluded.

Conclusions

Two global multistep mechanisms, the two-step mechanism by Westbrook and Dryer and the four-step mechanism by Jones and Lindstedt, have been tested and refined for oxy-fuel conditions, based on comparison with model predictions with a detailed chemical kinetic mechanism. In the modification, the initiation reactions involving the hydrocarbon fuel were unaltered. Changes were made in the $CO-CO_2$ reaction subset to obtain an improved fit for CO levels and steady state emissions as predicted by the detailed mechanism.

The modified schemes provide improved agreement with the detailed mechanism compared to the original mechanisms for isothermal plug flow reactor modeling under oxy-fuel combustion conditions. The improvement was most pronounced for WD mechanism, where the modified scheme yielded a better prediction of the peak and exit concentrations of CO. The modified JL mechanism offers a slight improvement in predicting CO trends.

A CFD analysis of a propane oxy-fuel flame was performed using both the original and modified mechanisms. The modified JL mechanism performed slightly better than the original, regarding CO predictions in the flame zone. The modified WD mechanism improved the prediction of CO especially in the post flame zone, but also a better temperature agreement with experimental data was obtained. In general, it is recommended to use the EDC turbulence chemistry interaction model, when modeling oxy-fuel flames. The traditional "mixed is burned" approach offered by the Eddy Dissipation Model is not likely to be applicable in a combustion system where the CO_2 dissociation can have a significant chemical effect.

Acknowledgment. This work was funded by Vattenfall Research and Development AB with Karin Eriksson as project manager. The authors would like to thank Anders Brink and W.P. Jones for helpful discussions.

EF8003619